Cancer Chemother Pharmacol (2007) 59:561–574
DOI 10.1007/s00280-006-0393-4

ORIGINAL ARTICLE

Sorafenib (BAY 43-9006) inhibits tumor growth and vascularization and induces tumor apoptosis and hypoxia in RCC xenograft models

Yong S. Chang · Jalila Adnane · Pamela A. Trail · Joan Levy · Arris Henderson · Dahai Xue · Elizabeth Bortolon · Marina Ichetovkin · Charles Chen · Angela McNabola · Dean Wilkie · Christopher A. Carter · Ian C. A. Taylor · Mark Lynch · Scott Wilhelm

Received: 14 August 2006 / Accepted: 9 November 2006 / Published online: 8 December 2006

Abstract
Purpose New research findings have revealed a key role for vascular endothelial growth factor (VEGF) in the stimulation of angiogenesis in clear cell renal carcinoma (RCC) which is a highly vascularized and treatment-resistant tumor. Sorafenib (BAY 43-9006, Nexavar®) is a multi-kinase inhibitor which targets receptor tyrosine and serine/threonine kinases involved in tumor progression and tumor angiogenesis. The effect of sorafenib on tumor growth and tumor histology was assessed in both ectopic and orthotopic mouse models of RCC.
Methods Sorafenib was administered orally to mice bearing subcutaneous (SC, ectopic) or sub-renal capsule (SRC, orthotopic) tumors of murine (Renca) or human (786-O) RCC. Treatment efficacy was determined by measurements of tumor volume and tumor growth delay. In mechanism of action studies, using the 786-O and Renca RCC tumor models, the effect of sorafenib was assessed after dosing for 3 or 5 days in the SC models and 21 days in the SRC models. Inhibition of tumor angiogenesis was assessed by measuring level of CD31 and α-smooth muscle actin (αSMA) staining by immunohistochemistry (IHC). The effect of sorafenib on MAPK signaling, cell cycle progression and cell proliferation was also assessed by IHC by measuring levels of phospho-ERK, phospho-histone H3 and Ki-67 staining, respectively. The extent of tumor apoptosis was measured by terminal deoxynucleotidyl transferase-mediated nick-end labeling (TUNEL) assays. Finally, the effects of sorafenib on tumor hypoxia was assessed in 786-O SC model by injecting mice intravenously with pimonidazole hydrochloride 1 h before tumor collection and tumor sections were stained with a FITC-conjugated Hypoxyprobe antibody.
Results Sorafenib produced significant tumor growth inhibition (TGI) and a reduction in tumor vasculature of both ectopic and orthotopic Renca and 786-O tumors, at a dose as low as 15 mg/kg when administered daily. Inhibition of tumor vasculature was observed as early as 3 days post-treatment, and this inhibition of angiogenesis correlated with increased level of tumor apoptosis (TUNEL-positive) and central necrosis. Consistent with these results, a significant increase in tumor hypoxia was also observed 3 days post-treatment in 786-O SC model. However, no significant effect of sorafenib on phospho-ERK, phospho-histone H3 or Ki-67 levels in either RCC tumor model was observed.
Conclusion Our results show the ability of sorafenib to potently inhibit the growth of both ectopically- and orthotopically-implanted Renca and 786-O tumors. The observed tumor growth inhibition and tumor stasis

Presented in part at the AACR-NCI-EORTC International Conference on Molecular Targets and Cancer Therapeutics, November 14–18, 2005, Philadelphia, PA, USA.

Y. S. Chang (✉) · J. Adnane · P. A. Trail · A. Henderson · D. Xue · E. Bortolon · M. Ichetovkin
Department of Protein Therapeutics,
Bayer Research Center, Bayer HealthCare, Pharmaceuticals,
400 Morgan Lane, West Haven, CT 06516, USA
e-mail: yong.chang.b@bayer.com

J. Levy · C. Chen · A. McNabola · D. Wilkie · C. A. Carter · I. C. A. Taylor · M. Lynch · S. Wilhelm
Department of Cancer Biology,
Bayer Research Center, Bayer HealthCare,
Pharmaceuticals, West Haven, CT, USA

or stabilization correlated strongly with decreased tumor angiogenesis, which was due, at least in part, to inhibition of VEGF and PDGF-mediated endothelial cell and pericyte survival. Finally, sorafenib-mediated inhibition of tumor growth and angiogenesis occurred at concentrations equivalent to those achieved in patients in the clinic.

Keywords Sorafenib · Multi-kinase inhibitor · Renal cell carcinoma · VEGF · Angiogenesis

Introduction

The median survival of renal cell carcinoma (RCC) patients with metastatic disease is approximately 8 months with a 5-year survival rate of below 10% [2, 10]. Traditional chemotherapy or hormonal therapy has been relatively ineffective, with only 10% of the patients showing response to these treatments [9, 28]. Cytokine therapy involving high-dose interleukin-2 (IL-2) or interferon-α (IFN-α) has also yielded limited benefit, with objective response rates of only 15% for both [27]. Thus, there is a high medical need for new effective therapies for RCC. A hallmark of RCC is the frequent loss of the von Hippel-Lindau (VHL) tumor suppressor gene, which is a key regulator of hypoxia inducible factor-1α (HIF-1α) [10, 13, 15] and vascular endothelial growth factor (VEGF) production [29]. Loss of VHL results in the upregulation of VEGF production and induction of tumor angiogenesis [24].

A number of new agents, designed to block tumor signaling pathways and inhibit tumor angiogenesis, have shown promise in clinical trials in RCC [2, 27, 31]. The first of these agents approved for the treatment of advanced RCC is sorafenib (BAY 43-9006, Nexavar®), a small molecule kinase inhibitor of the vascular endothelial growth factor receptor (VEGFR). More recently, sunitinib (SU11248, Sutent®), also a small molecule kinase inhibitor with activity against the VEGFR, was approved for the treatment of advanced RCC. Sorafenib is an orally active, multi-kinase inhibitor that targets the serine/threonine kinases RAF (RAF-1 and B-RAF) and as well as receptor tyrosine kinases (VEGFR-1, -2 & -3 and platelet derived growth factor receptor-β (PDGFR-β)), which play key roles in tumor growth and angiogenesis. Sorafenib has been tested in patients with advanced RCC in a large multi-center placebo-controlled phase III trial [11, 16]. Interim results of this trial showed that patients receiving sorafenib had a 39% increase in overall survival, as compared to placebo. The median survival for the placebo group was 14.7 months while the median survival for patients receiving sorafenib had not yet been reached [11]. Thus, there is hope that these new agents will significantly improve the clinical outcome for RCC patients and, to maximize their clinical benefit we need to have a thorough understanding of their mechanism of action.

We and the others have previously shown that sorafenib exhibits a broad spectrum activity against human xenograft models of multiple histological types including, breast, colon, thyroid, melanoma and lung [7, 32, 35]. Inhibition of RAF/MEK/ERK pathway correlated with tumor growth inhibition in some, but not all, tumor models. Indeed, in some xenograft models, sorafenib mediated potent anti-tumor effects without affecting MAPK signaling. Therefore, depending on the tumor type, sorafenib's mechanism of action may be mediated through either its effect on angiogenesis or tumor proliferation or a combination of both.

In the present study, the anti-tumor activity and the mechanism of action of sorafenib in subcutaneous (SC) and sub-renal capsule (SRC) models of a human (786-O) and murine (Renca) RCC was investigated.

Materials and methods

Compound and vehicle

BAY 54-9085 (MW 637), a tosylate salt of BAY 43-9006 (MW 464.7), was used in all studies. The compound was synthesized at Bayer HealthCare, Pharmaceuticals (West Haven, CT, USA). The equivalent dose of the free base BAY 43-9006 used in these studies is reported. BAY 54-9085 was formulated at 4-fold (4×) of the highest dose in a Cremophor EL/Ethanol (50:50) solution. This 4× stock solution was prepared fresh daily. Final dosing solutions were prepared on the day of use by dilution to 1× with endotoxin-free distilled water (GIBCO, Grand Island, NY, USA) and mixed by vortexing immediately prior to dosing. Lower doses were prepared by dilution of the 1× solution with Cremophor EL/Ethanol/water (12.5:12.5:75).

Tumor cell lines

The Renca murine (wild type VHL; [26]) was obtained from the NCI. The human RCC cell line, 786-O ($VHL^{-/-}$; [3]) was obtained from American type culture collection (ATCC). All cell lines were maintained and propagated in RPMI 1640 media (GIBCO) supplemented with 10% heat-inactivated fetal bovine serum (JRH Biosciences, Lenexa, KS, USA) at 37°C and 5% CO_2.

In vivo experiments with subcutaneous tumors

Female athymic NCr *nu/nu* mice (Taconic Farms, Germantown, NY, USA) were implanted subcutaneously with 5×10^6 Renca cells or with 1 mm^3 786-O tumor fragments. Mice were housed at Bayer Corporation in accordance with Bayer IACUC, State, and Federal guidelines for the humane treatment and care of laboratory animals. Mice received food and water ad libitum. Treatment began when tumors reached a volume of 100 mm^3. Sorafenib or vehicle control was administered orally, once a day, for 9 or 21 days in Renca and 786-O models, respectively, at dose levels of 90, 60, 30, or 15 mg/kg/dose. Tumor size was calculated using the equation $(l \times w^2)/2$, where l and w refer to the larger and smaller dimensions collected at each measurement. Efficacy was measured as percent tumor growth inhibition (TGI) relative to vehicle-treated group. TGI is calculated by the equation $[1 - (T/C)] \times 100$, where T and C represent the mean tumor mass on the last day of therapy in the sorafenib-treated (T) and vehicle control (C) groups, respectively. A TGI of >50% is considered efficacious. Error bars were calculated as the standard error of the means. The general health of mice was monitored daily. Tumor dimensions and body weights were recorded two to three times a week starting with the first day of treatment.

To determine the mechanism of action of sorafenib in these RCC models, a separate experiment was designed in which drug treatment was initiated when tumors averaged 200–400 mm^3. Sorafenib and control vehicle were administered orally, once a day, for 3 or 5 days at dose levels of 60 and 30 mg/kg in 786-O tumor model and 90, 60, 30, and 15 mg/kg/dose in Renca tumor model. Three hours after the last dose, tumors were removed and fixed in 10% formalin and embedded in paraffin for immunohistochemical (IHC) analysis.

In vivo experiments with sub-renal capsule (SRC)-implanted tumors

One mm^3 tumor fragments of Renca or 786-O tumors were implanted in the SRC of individual male athymic nude mice (NCr-*nu/nu*; Taconic Farms) by making an incision in the renal capsule and placing the donor tumor fragment underneath the capsule sheath. Sorafenib and control vehicle were administered orally, once a day, for 10 or 21 days in Renca and 786-O models, respectively, at dose levels of 60 and 30 mg/kg in 786-O tumor model and 90, 60, 30, and 15 mg/kg/dose in Renca tumor model. At the end of treatment, the mouse kidneys were removed and surface photomicrographs were taken using a Spot Jr. camera (Diagnostic Instruments, USA) attached to a Nikon stereomicroscope. Tumors were then fixed in 10% formalin and embedded in paraffin for IHC analysis.

Immunohistochemistry

Immunostaining of paraffin-embedded tumor sections ($n = 3$ tumors) was performed with an anti-CD31 mouse antibody (PECAM-1 (M-20), Santa Cruz Biotechnology, Santa Cruz, CA, USA) diluted 1:750 or, as a negative control, with a goat IgG antibody (Jackson ImmunoResearch Laboratories, Inc., West Grove, PA, USA). Detection of αSmooth Muscle Actin (αSMA), was performed with an anti-αSMA mouse antibody (DAKO Cytomation) diluted 1:100. The level of phospho-ERK1/2 was determined using an anti-pERK1/2 antibody (phospho-p44/42; Cell Signaling Technology, Inc. Danvers, MA, USA) diluted 1:100. The proliferation index in Renca tumors was determined by staining tumor sections with an anti-phospho histone H3 antibody (Phospho-histone H3 (Ser10), Cell Signaling Technology) diluted 1:100. Similarly, the proliferation index in 786-O tumor was determined by staining tumor sections with an anti-Ki-67 antibody (Zymed Laboratories) diluted 1:50. The extent of apoptosis in the tumors was measured by TUNEL using the TdT-Fragel DNA Fragmentation detection Kit (Calbiochem), following the manufacturer's protocol. The slides were counterstained with Mayer's hematoxylin.

Tumor hypoxia was determined using Hypoxyprobe-1 Plus Kit in which, 1 h before tumor collection, mice were injected intravenously with Hypoxyprobe TM-1 [pimonidazole hydrochloride, 60 mg/kg; (Chemicon International; Temecula, CA, USA)]. Tumors were harvested 4 and 24 h after the last dose of sorafenib, which was dosed once-a-day for 3 days at 15 and 30 mg/kg. For UV visualization, formalin-fixed, paraffin-embedded tumor sections cut at 5 μm were incubated for 1 h with the FITC-conjugated Hypoxyprobe-1 primary antibody supplied with the kit (Hypoxyprobe-1 Plus Kit; Chemicon International). Sections were also incubated with a goat anti-CD31 Ab (Santa Cruz Biotechnology).

Fluorescent dual staining of endothelial cells and pericytes was carried out using a rat monoclonal anti-CD34 antibody at a dilution of 1:50 (Abcam) and a murine anti-SMA antibody at a dilution of 1:100 (Dako). Slides were then incubated with a goat anti-rat AlexaFluor 488 (CD34) and with a donkey anti-mouse AlexaFluor 555 (αSMA) and detected using FITC and Texas Red filters, respectively.

Quantification of microvessels with CD31 and αSMA

Tissue sections from three different tumors were viewed using an ×10 objective magnification (0.644 mm^2 per field). Greater than ten fields per section were randomly analyzed, excluding peripheral surrounding connective tissue and central necrotic tissue. The slides were coded before analysis. CD31- and αSMA-positive areas were quantified using the software ImagePro Plus version 3.0 (Media Cybernetics, Silver Spring, MD, USA) and SIS image analysis software (Soft Imaging Systems, GmbH, Germany), respectively. The data is presented as percentage of microvessel area (MVA, %). Data were analyzed statistically with one-way ANOVA (GraphPad PRISM, version 3.03; GraphPad Softwares, Inc., San Diego, CA, USA) or with two-tail student's *t* test. A value of $P < 0.05$ was considered significant.

Results

Anti-tumor efficacy and mechanism of action of sorafenib in human 786-O and murine Renca renal sub-cutaneous tumor models

Athymic mice were implanted subcutaneously with 786-O ($VHL^{-/-}$; [3]) tumor fragments and treatment with sorafenib or vehicle control was initiated on day 13 when tumors averaged 100 mm^3 in size. As shown in Fig. 1a, daily treatment with sorafenib produced dose-dependent inhibition of 786-O tumor growth. At a dose of 15 mg/kg, 28% tumor growth inhibition was observed, while treatment with 30, 60 or 90 mg/kg doses resulted in a greater inhibition of tumor growth (80%) with tumor stabilization at the 60 and 90 mg/kg doses (Fig. 1a). Similar to 786-O model, sorafenib produced dose-dependent inhibition of tumor growth in the Renca tumor model (Fig. 1b). At a dose of 15 mg/kg, 53% tumor growth inhibition was observed, while treatment with 60 and 90 mg/kg doses produced 82% inhibition of tumor growth and resulted in tumor stabilization during treatment. These results show that sorafenib is highly efficacious and induced tumor stasis or stabilization in two RCC models (786-O and Renca) when implanted subcutaneously.

To better understand the mechanism of action of sorafenib in vivo, mice bearing SC 786-O tumors (~200 mm^3) were treated for 3 or 5 days with vehicle control or sorafenib at dose levels of 30 or 60 mg/kg. Tumors were excised 3 h after the last treatment and analyzed in multiple assays. To determine the effect of sorafenib on MAPK signaling pathway and tumor proliferation, 786-O tumor sections were analyzed for phospho-ERK (pERK) and Ki-67 by immunohistochemistry (IHC). Representative photomicrographs of pERK and Ki-67 staining are illustrated in Fig. 2a and b, which show no detectable changes in these markers in response to sorafenib. Similar results were obtained in the Renca ($VHL^{+/+}$; [26]) tumor model, in that no

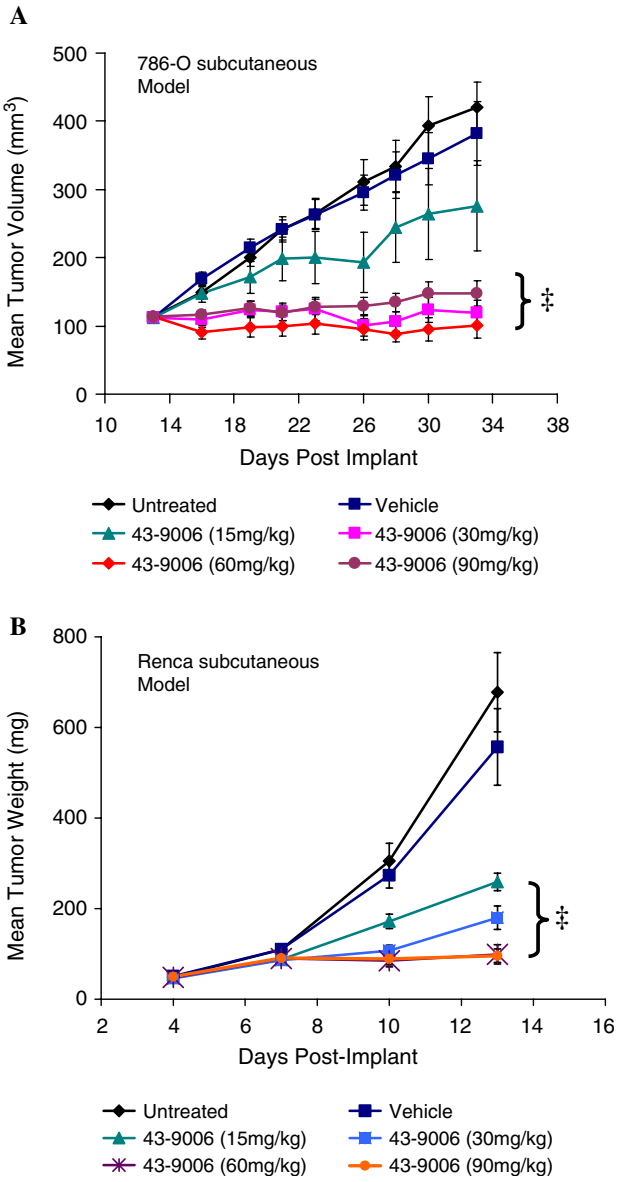

Fig. 1 Sorafenib inhibits the growth of subcutaneously implanted human 786-O and murine Renca RCC tumors. Female athymic NCr *nu/nu* mice were implanted subcutaneously with 1 mm^3 786-O tumor fragments (**a**) or 5×10^6 Renca cells (**b**). Treatment began when tumors reached a volume of 100 mm^3. Sorafenib or vehicle control was administered orally, once a day, for 21 days (786-O) or 9 days (Renca) at the indicated dose. Percent tumor growth inhibition was calculated relative to vehicle control group. In both 786-O and Renca models, sorafenib exhibited significant tumor growth inhibition. $N = 10$ per group. $^{\ddagger}P < 0.001$

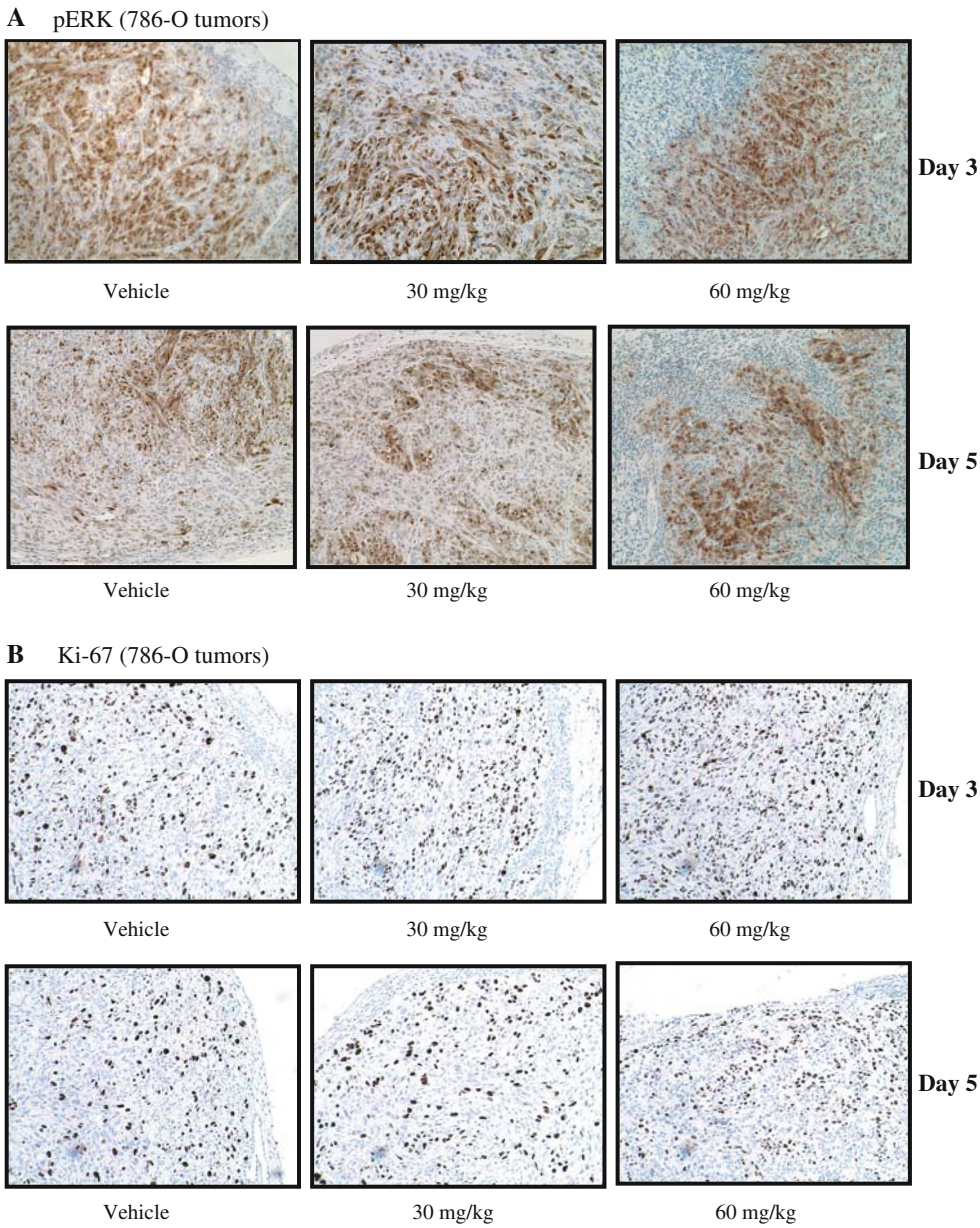

Fig. 2 Sorafenib did not alter the level of phospho-ERK or Ki-67 in 786-O tumors. Female athymic NCr *nu/nu* mice were implanted subcutaneously with 1 mm^3 786-O tumor fragments. Treatment began when tumors reached a volume of 200–400 mm^3. Sorafenib and vehicle control were administered orally, once a day, for 3 or 5 days at the indicated dose. Three hours after the last dose, tumors were removed and processed for immunohistochemical analysis, as described in Materials and methods. Tumors were stained for **a** phospho-ERK (pERK)or **b** Ki-67 using DAB chromagen and representative photographs were taken using bright-field microscopy (×10). There was no significant change in pERK or Ki-67 in sorafenib-treated tumors compared to those treated with vehicle

effect of sorafenib on pERK or phospho-histone-H3, a marker of cell proliferation, was observed (data not shown). Thus, in both RCC models, there was no correlation between tumor growth inhibition and inhibition of MAPK signaling or tumor cell proliferation. The lack of effect on Ki-67 and phospho-histone-H3, proliferation markers suggests that sorafenib-mediated tumor growth inhibition is unlikely to be due to inhibition of cancer cell proliferation. Alternative mechanisms, such as inhibition of angiogenesis and induction of apoptosis, appear to be responsible for the anti-tumor efficacy observed with sorafenib. Similarly, the lack of effect on tumor cell MAPK signaling in situ in 786-O sorafenib-treated tumors is consistent with the modest inhibition observed when 786-O cells are treated in vitro with sorafenib with IC_{50} = 15–20 μM in MAPK signaling (as measured by phospho-ERK and phospho-MEK) (data not shown).

Since no detectable changes in pERK and tumor cell proliferation markers (Ki-67 and phospho-histone-H3) were observed, we analyzed the effect of sorafenib treatment on inhibition of tumor vasculature markers by staining the 786-O tumor sections with an anti-CD31 (Fig. 3a) and anti-αSMA (Fig. 3b) antibodies. In the vehicle-treated tumors, the expression level of CD31 and αSMA angiogenic markers was remarkably high, as compared to other tumor xenograft models we have previously used. In this 786-O model, both VHL and HIF-1α are absent. However, it has been shown by Shinojima et al. [33] that renal cancer cells lacking

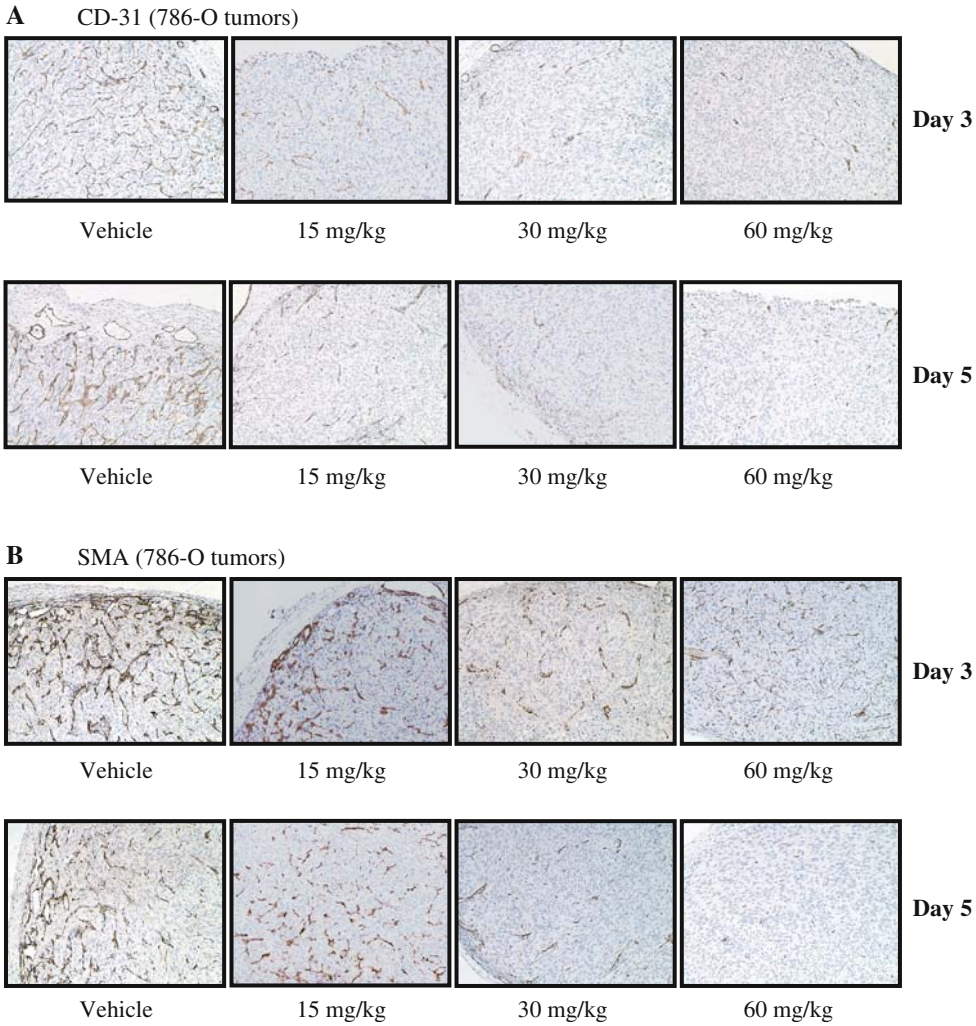

Fig. 3 Sorafenib inhibits the vascularization of VHL$^{-/-}$ 786-O tumors. Female athymic NCr *nu/nu* mice were implanted subcutaneously with 1 mm^3 786-O tumor fragments. Treatment began when tumors reached a volume of 200–400 mm^3. Sorafenib and vehicle control were administered orally, once a day, for 3 or 5 days at the indicated dose. Three hours after the last dose, tumors were removed and processed for immunohistochemical analysis, as described in Materials and methods. Tumors were stained for CD31 **(a)** or αSMA **(b)** using DAB chromagen and representative photographs were taken using bright-field microscopy (×10). **c** Dual staining of tumors for CD34 (*green*, FITC) (endothelial cells) and αSMA (*red, Texas Red*) (pericytes) using fluorescent microscopy (×40). A significant decrease of the angiogenic markers (CD34 and αSMA) occurred within the tumor, with endothelial cells showing greater sensitivity than pericytes to sorafenib treatment. The level of CD34 and αSMA in the 786-O tumors **(d)** and Renca tumors **(e)** was evaluated on images captured using bright-field microscopy (×10 magnification). Results shown are average of over ten random tumor sections taken from three different tumor samples. Significant inhibition of tumor vasculature occurred in response to sorafenib treatment. $^{*}P < 0.05$, $^{\dagger}P < 0.01$, and $^{\ddagger}P < 0.001$

HIF-1α expression maintain VEGF expression through HIF-2α. In HIF-1α defective RCC cell lines, the knockdown of the HIF-2α gene completely abolished VEGF production, irrespective of the VHL gene mutation status.

As shown in Fig. 3a and b, a significant reduction in 786-O tumor vasculature was evident within 3 days of sorafenib treatment at 15, 30 and 60 mg/kg. Moreover, tumor sections were co-stained for both anti-CD31 (endothelial cell marker) and anti-αSMA (pericyte marker) (Fig. 3c). Consistent with results obtained using bright-field microscopy (Fig. 3a, b), fluorescent microscopy results highlight the efficacy of sorafenib in decreasing the level of CD31 and αSMA vascular markers. Interestingly, compared to smooth muscle cells, endothelial cells seem to be more sensitive to sorafenib treatment, as demonstrated by the strong decrease of CD34 staining at a dose as low as 15 mg/kg. The extensive degree of vascularization of 786-O tumors was demonstrated by quantifying the level of CD31 and αSMA in tumor sections, which produced a mean vessel area (MVA) of approximately 8–10% of

Fig. 3 contiuned

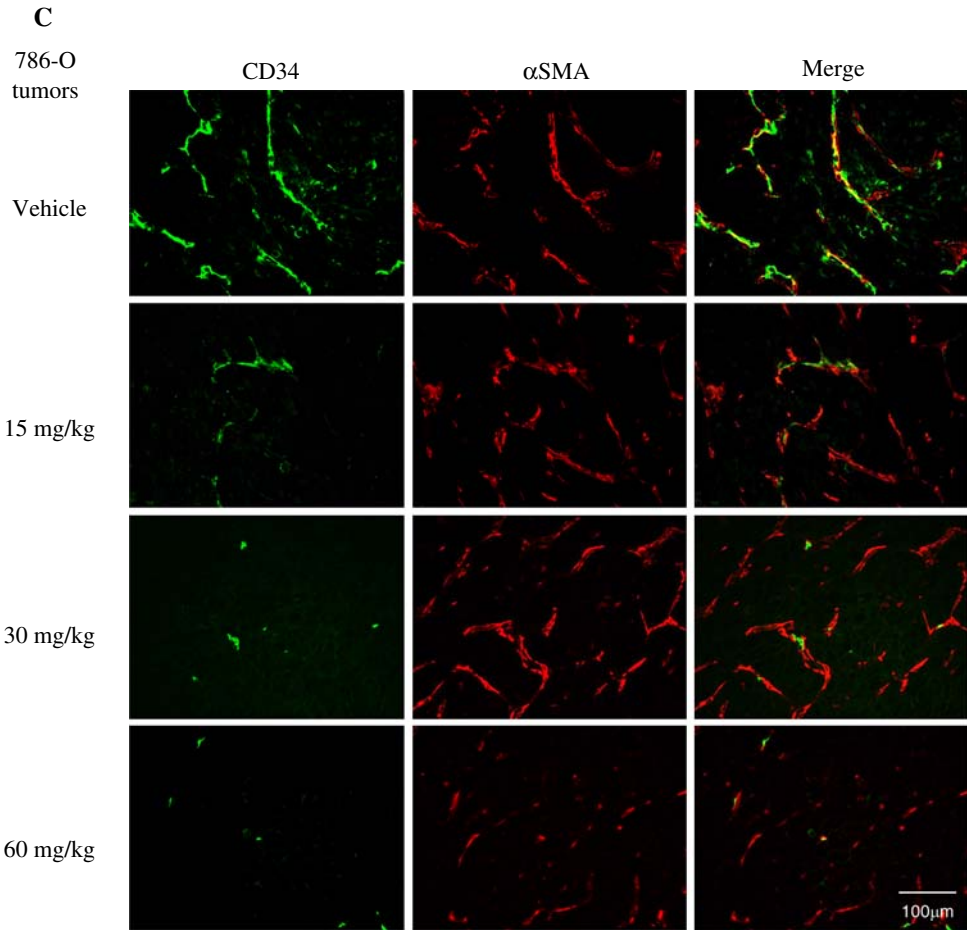

the total tumor area (Fig. 3d). The MVA, as measured by the level of CD31 staining, was decreased by 70% ($P < 0.05$) at 15 mg/kg dose and 90% ($P < 0.01$) at 30 and 60 mg/kg dose and thus, representing less than 1% of the total tumor area in response to three doses of sorafenib. Similarly, treatment with sorafenib for 5 days at 30 and 60 mg/kg resulted in a decrease of MVA by 75 and 88% ($P < 0.01$), respectively. The effect of sorafenib on αSMA was less dramatic, as compared to CD31 but, nevertheless, was significant ($P < 0.05$). Indeed, on day 3, sorafenib treatment at 30 and 60 mg/kg resulted in a decrease of αSMA level by 48% ($P < 0.05$) and 64% ($P < 0.01$), respectively. However, when treatment was extended to 5 days, a greater decrease of αSMA level was observed, 68% ($P < 0.05$) and 88% ($P < 0.01$) at 30 and 60 mg/kg, respectively.

As shown in Fig. 3e, similar results were obtained in the Renca murine model. Significant inhibition of MVA ($P < 0.001$), as measured by either anti-CD31 or anti-αSMA, was seen at all doses tested. For instance, a dose of 15 mg/kg produced an 81% reduction in MVA, while higher doses of 30, 60 and 90 mg/kg produced 89% inhibition ($P < 0.001$). A more pronounced dose-response was seen when MVA was assessed via αSMA. Indeed, doses of 15, 30, 60 and 90 mg/kg decreased the MVA by 58, 79, 92 and 90%, respectively ($P < 0.001$).

Next, the effect of sorafenib on tumor hypoxia levels in 786-O SC model was measured using pimonidazole hydrochloride, as described in Materials and methods. Tumor samples were collected at 4- and 24-h time-points after 3 days of treatment at doses of 15 and 30 mg/kg. As shown in Fig. 4, tumor areas with no detectable CD31 (red) stained positively for hypoxia (green). The reduction in tumor vasculature (decrease of CD31 and αSMA staining) (Fig. 3a–e) and increase of tumor hypoxia (increase of Hypoxyprobe staining) (Fig. 4) correlated with a significant increase in apoptosis and necrosis, as evidenced by the extensive area staining positive for TUNEL (Fig. 5a, b). Significant increase in TUNEL-positive area was observed at all doses examined ($P < 0.05$). Indeed, a 3-day treatment at a dose of 30 or 60 mg/kg resulted in an increase of TUNEL-positive area by 17.7 and 28.9% ($P < 0.05$), respectively, and, a prolonged treatment of 5 days resulted in 31.3 and 40.8% ($P < 0.01$), respectively (Fig. 5b). Thus, the degree of tumor apoptosis appears

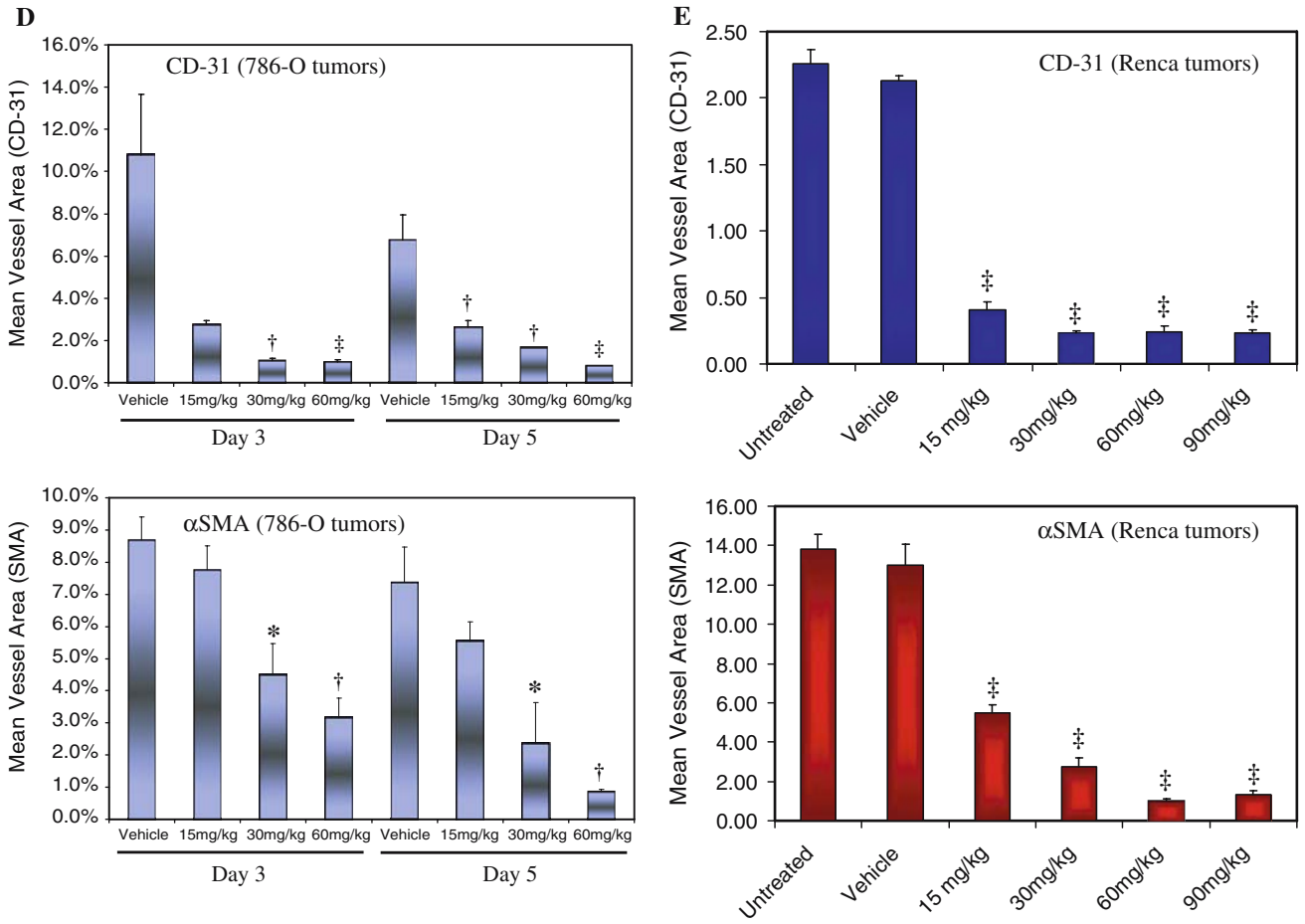

Fig. 3 contiuned

to be both dose- and time-dependent. This increase in TUNEL positive staining is most likely a secondary effect of inhibiting tumor angiogenesis as sorafenib did not induce apoptosis in vitro in this cell line (data not shown).

Anti-tumor efficacy and mechanism of action of sorafenib in Renca and 786-O RCC orthotopic models

We sought to determine whether the site of tumor implantation would alter the sensitivity to sorafenib or its mechanism of action in Renca and 786-O models (Fig. 6). To this end, fragments of 786-O and Renca tumors, which were propagated serially as SC tumors in mice, were implanted orthotopically under the SRC. As in Renca and 786-O SC models, sorafenib was highly effective in inhibiting the growth of both 786-O (Fig. 6a) and Renca renal tumor orthotopic models (Fig. 6c). Representative kidney photomicrographs of the 786-O and Renca SRC model are shown in Fig. 6a and c. Sorafenib-treated tumors were noticeably smaller and opaque, displaying weak vasculature, relative to control tumors, which were large, virtually overwhelming the kidney, vibrant in color and highly vascularized. IHC analysis of CD31 and αSMA staining in sorafenib-treated tumors confirmed the apparent decrease in vasculature. As shown in Fig. 6b, significant reduction in the levels of CD31 and αSMA angiogenic markers was observed. Noteworthy, sorafenib had no effect on the vasculature, as measured by CD31 staining, of adjacent normal kidney tissue (Fig. 6b). Similar to 786-O model, the Renca RSC model showed a significant decrease of CD31 and αSMA angiogenic markers in response to sorafenib (Fig. 6d). As shown in Fig. 6d, quantification of the microvessel area in the tumor tissue, using the CD31 marker, showed a significant inhibition of angiogenesis (69%, $P < 0.001$) at doses as low as 15 mg/kg. A more pronounced decrease of CD31 level (87%, $P < 0.001$) was observed at the 30 mg/kg dose. Increasing the treatment dose to 60 or 90 mg/kg did not achieve a higher inhibition than the one seen at the 30 mg/kg dose. Similar to results obtained with CD31, sorafenib significantly decreased the level of αSMA (Fig. 6d). Treatment at doses of 60 and 90 mg/kg

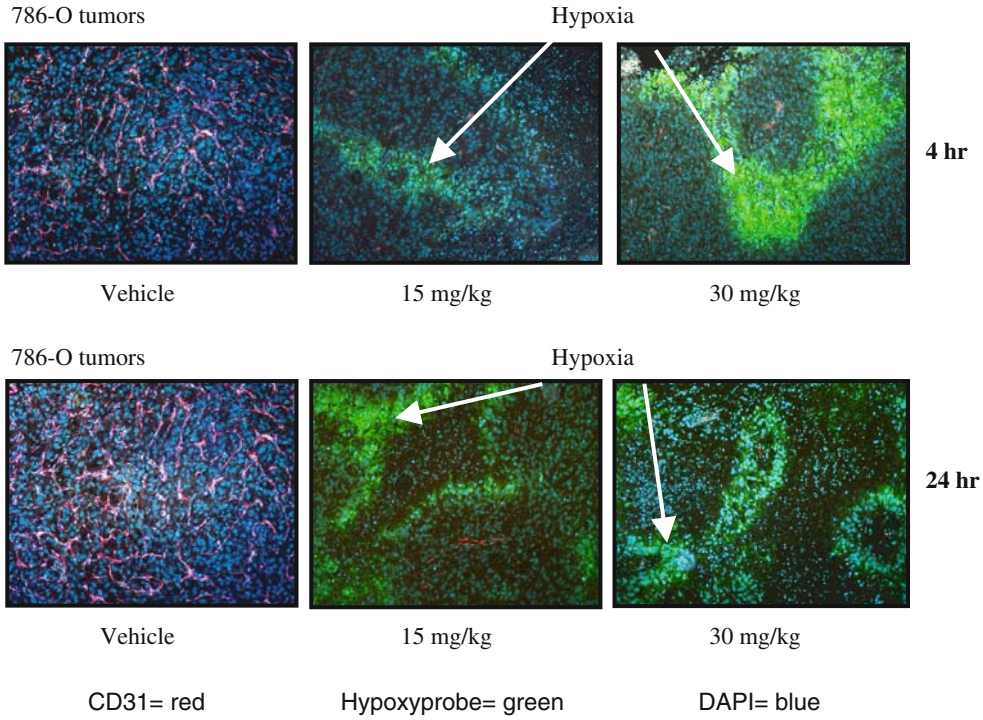

Fig. 4 Sorafenib strongly induced tumor hypoxia. Following 3 days of treatment with sorafenib at the indicated dose, mice were injected with HypoxyprobeTM-1 (pimonidazole hydrochloride, 60 mg/kg), as described in Materials and methods. Tumor sections were stained with FITC-conjugated Hypoxyprobe-1 antibody to detect hypoxic tissue. Sections were also stained for CD31 (*Red*) and DAPI (*Blue*). Tumor hypoxia is evident at both l5 and 30 mg/kg dose regimens

resulted in 74 and 60% decrease of αSMA ($P < 0.001$), respectively.

Next the effect of sorafenib on MAPK signaling pathway and tumor proliferation in SRC tumors, phospho-ERK and Ki-67 levels were evaluated. Similar to results obtained in 786-O sub-cutaneous model, no detectable change in phospho-ERK or Ki-67 levels were observed in 786-O SRC tumors (Fig. 7). This in situ result is consistent with the modest effects observed with sorafenib in vitro for 786-O cells. Taken together, our results show that tumor growth inhibition mediated by sorafenib in SC and SRC models of RCC is due to inhibition of tumor angiogenesis rather than inhibition of the MAPK signaling in RCC tumors.

Discussion

RCC is characterized by the loss of VHL tumor suppressor protein resulting in dysregulation of growth factor signaling including, VEGF, PDGF-β, and TGF-α, as well as dysregulation of Raf pathways, which play key roles in angiogenesis, lymphangiogenesis, tumor growth and survival [10, 13, 15, 29, 34]. Results described in this report show the ability of sorafenib to potently inhibit tumor growth and tumor angiogenesis of RCC tumors in both ectopic and orthotopic tumor models at dose levels that produced plasma drug concentrations within the range observed in patients receiving the standard dose of 400 mg/b.i.d. The mean AUC in patients receiving sorafenib at 400 mg/b.i.d. continuously for 7 days is 121.7 μM h [8] which is within the range of the observed mouse plasma AUC seen at doses of 10 mg/kg (62 μM h) and 30 mg/kg (210 μM h) (data not shown). The robust efficacy observed in RCC models is consistent with previously reported results, showing the high efficacy of sorafenib in multiple human tumor xenograft models [35]. Sorafenib is a multi-kinase inhibitor that targets several receptor tyrosine kinases including, VEGFR-1, -2 &-3 and PDGFR-β, and serine threonine kinases including, Raf-1 and B-Raf, all shown to be involved in neovascularization and tumor progression. We and others have shown the ability of sorafenib to inhibit the MAPK pathway in situ in tumor models of multiple tumor types [7, 25, 30, 32, 35]. However, not all tumor models showed an inhibition of MAPK pathway, even though sorafenib was very efficacious in inhibiting tumor growth, suggesting that sorafenib-mediated tumor growth inhibition can occur in a MAPK-independent manner [35]. In the RCC models, we did not observe a change in ERK phosphorylation in response to sorafenib in neither Renca nor 786-O RCC tumors whether they were implanted ectopically nor orthotopically. Furthermore, proliferation markers, such as phospho-histone H3 and Ki-67, remained essentially unchanged following sorafenib treatment. Therefore, inhibiting tumor proliferative signals is not the primary mechanism of action of sorafenib in these renal tumor models. In contrast, a strong reduction in tumor angio-

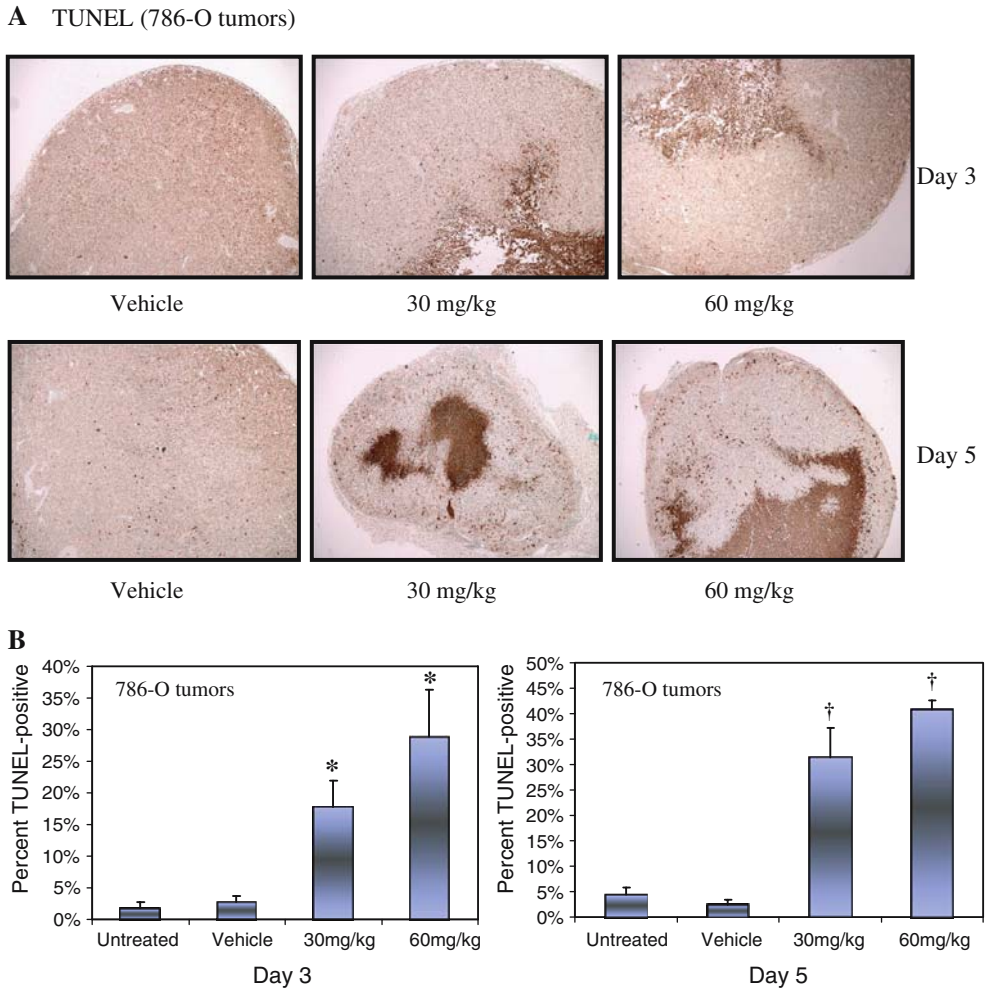

Fig. 5 Sorafenib induces tumor apoptosis and necrosis in the 786-O xenograft model. Female athymic NCr *nu/nu* mice were implanted subcutaneously with 1 mm^3 786-O tumor fragments. Treatment began when tumors reached a volume of 200–400 mm^3. Sorafenib and vehicle control were administered orally, once a day, for 3 or 5 days at the indicated dose. Three hours after the last dose, tumors were removed and processed for immunohistochemical analysis, as described in Materials and methods. **a** Representative photographs of the 786-O tumors are shown (×4). **b** The extent TUNEL-positive area in the 786-O tumors was evaluated on images captured using bright-field microscopy (×4 magnification). Results shown are average of over ten random tumor sections taken from three different tumor samples. Significant induction of apoptosis is observed at day 3 at all doses examined and getting more pronounced at day 5. $^{*}P < 0.05$ and $^{\dagger}P < 0.01$

genesis was observed in both the ectopic and orthotopic models of 786-O and Renca RCC, resulting in tumor stabilization. Thus, inhibition of tumor angiogenesis seems to be a predominant mechanism of action of sorafenib in these highly vascularized RCC models, leading to tumor growth inhibition.

The high sensitivity of Renca $VHL^{+/+}$[26] and 786-O $VHL^{-/-}$ [3] tumors to a multi-kinase and anti-angiogenesis inhibitor, such as sorafenib, confirms the key role of angiogenesis in supporting RCC tumor growth. Angiogenesis involves the interaction of multiple growth factors, including VEGF, angiopoietin-1 (Ang-1), basic fibroblast growth factor (bFGF), and PDGF [12]. During the initial phase of angiogenesis, or sprouting, endothelial cells are highly dependent on

Fig. 6 Sorafenib inhibits tumor growth and vascularization in the 786-O and Renca orthotopic tumor model. **a** Representative photomicrographs of kidneys harboring 786-O tumors are shown**.** Sorafenib-treated tumors, which were implanted in the sub-renal capsule, are noticeably smaller and opaque, displaying little vasculature relative to vehicle control tumors. **b** Representative photographs of the 786-O orthotopic tumors are shown (×10 magnification). Sorafenib decreased the level of both CD31 and αSMA angiogenic markers in the tumors. Note that sorafenib did not alter the adjacent vasculature of the normal kidney tissue. **c** Representative photomicrographs of kidneys harboring Renca tumors are shown**.** Sorafenib-treated tumors, which were implanted in the sub-renal capsule, are noticeably smaller and opaque, displaying little vasculature relative to vehicle control tumors. **d** Analysis of CD31 and αSMA levels in Renca orthotopic tumors after treatment with sorafenib. Results shown are average of over ten random tumor sections taken from three different tumor samples. Significant inhibition of tumor vasculature was observed in response to treatment. $^{\dagger}P < 0.01$, and $^{\ddagger}P < 0.001$ ▶

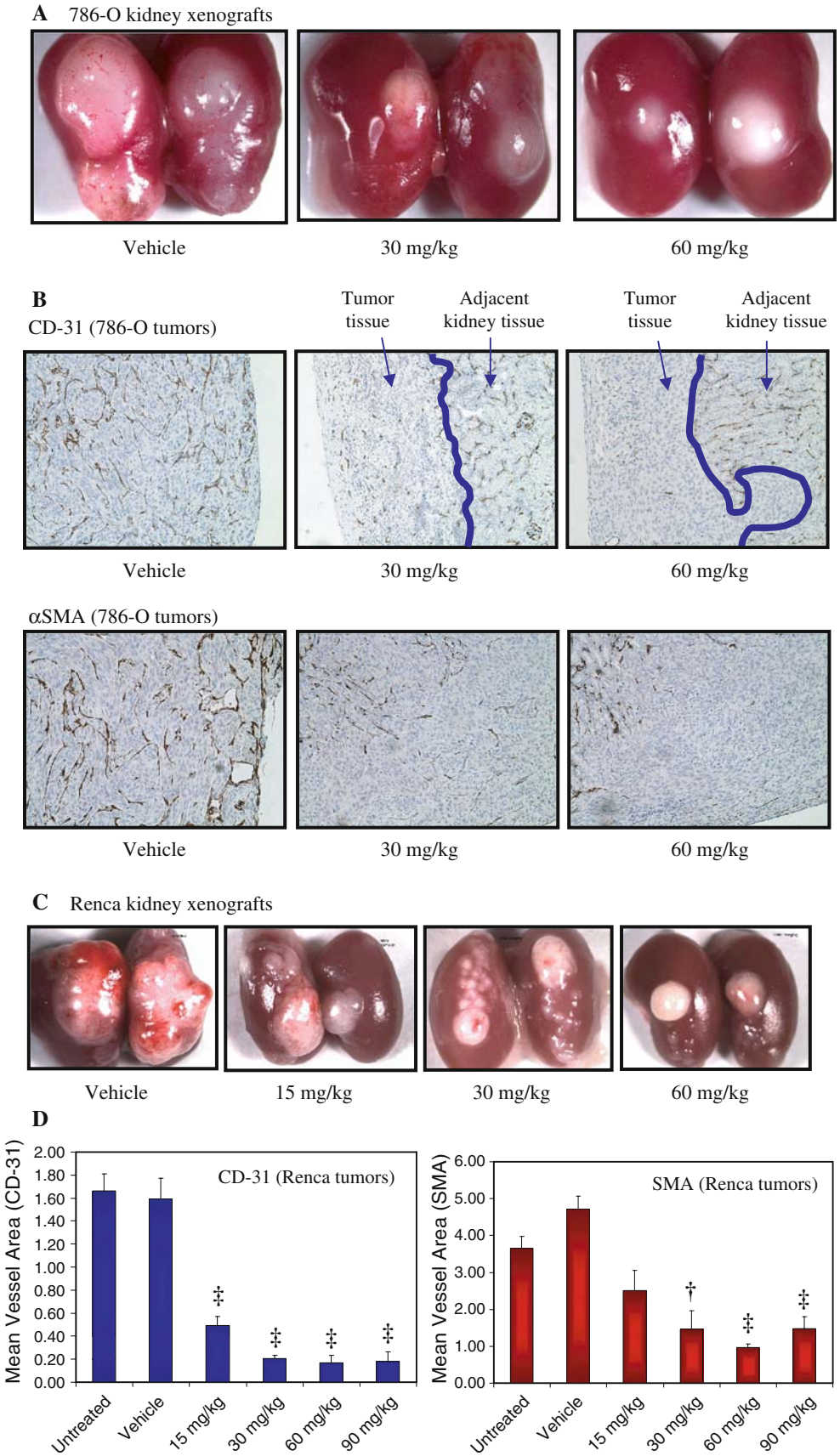
A 786-O kidney xenografts
Vehicle
30 mg/kg
60 mg/kg
B
CD-31 (786-O tumors)
Tumor tissue
Adjacent kidney tissue
Tumor tissue
Adjacent kidney tissue
Vehicle
30 mg/kg
60 mg/kg
αSMA (786-O tumors)
Vehicle
30 mg/kg
60 mg/kg
C Renca kidney xenografts
Vehicle
15 mg/kg
30 mg/kg
60 mg/kg
D
Mean Vessel Area (CD-31)
CD-31 (Renca tumors)
Untreated
Vehicle
15 mg/kg
30 mg/kg
60 mg/kg
90 mg/kg
Mean Vessel Area (SMA)
SMA (Renca tumors)
Untreated
Vehicle
15 mg/kg
30 mg/kg
60 mg/kg
90 mg/kg

growth factors such as VEGF for survival. As the process continues, newly formed vessels begin to stabilize and recruit pericytes, and subsequently become less dependent on growth factors for survival. Stabilization and maturation of newly formed blood vessels are thought to be mainly mediated by angiopoietin-1 (ang-1) and PDGF [5, 17, 21]. In hypoxic tumors, because there is continuous production of hypoxia-induced angiogenic factors, newly formed vessels do not fully mature and are under constant transition between stabilized and de-stabilized states. As demonstrated by Benjamin et al. [4] using the tetracycline-off-VEGF C6 glioma xenograft system, the removal of VEGF results in selective ablation of only immature vessels leaving mature vessels intact. Recently, Bergers et al. [6] demonstrated the advantage of targeting both endothelial cells and pericytes. Using the RIP1Tag2 transgenic mice, they were able to demonstrate that the combinations of SU5416 (VEGFR-2 inhibitor) with either SU6668 or imatinib, which both have potent PDGFR activity, showed greater anti-tumor activity than either single agent alone at all stages of islet cell carcinogenesis. This is consistent with reported findings involving VEGF in the initiation and promotion of endothelial cell proliferation and survival while PDGF mainly acts to stabilize vessels by promoting pericyte recruitment and maturation [5, 6]. Sorafenib possesses a potent activity against both VEGFR-2 ($IC_{50} = 20$ nM) and PDGFR-β ($IC_{50} = 53$ nM) [35]. By combining both VEGFR-2 and PDGFR-β inhibitory activity into one single molecule, sorafenib provides one avenue to improve anti-angiogenesis therapy by targeting both endothelial cells as well as their supporting pericytes.

In this report, we show that sorafenib mediates the inhibition of both immature and mature tumor vessels, as measured by CD31 (endothelial cells) and αSMA (pericytes) staining, respectively. It is important to note that sorafenib did not alter CD31 and αSMA staining in the normal kidney tissue, showing the resistance of well-established and stable vessels to sorafenib. Thus, it appears that inhibiting multiple signaling pathways (VEGFR and PDGFR) supporting tumor angiogenesis is more advantageous than inhibiting a single target or signaling pathway. As previously reported by Wilhelm et al. [35], sorafenib was initially discovered as a potent Raf kinase inhibitor and, several lines of evidence point to a role of RAF1 in the regulation of endothelial cell survival [1, 18]. We were unable to demonstrate any induction of endothelial cell apoptosis in CD31 positive cells in the 786-O treated tumors

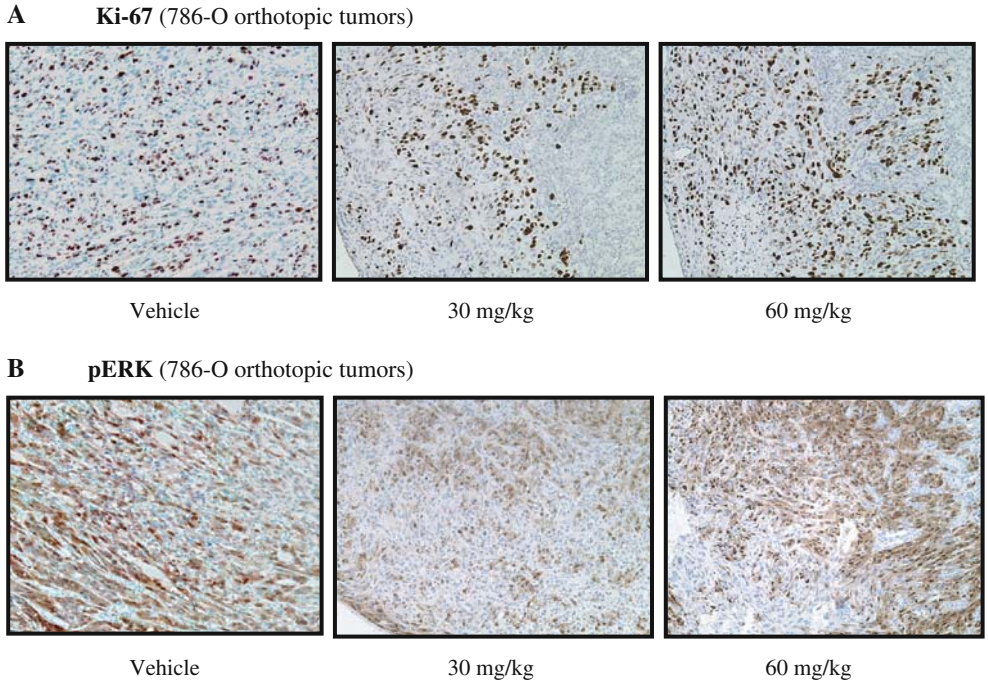

Fig. 7 Sorafenib did not alter the level of Ki-67 or phospho-ERK in 786-O orthotopic tumors. Mice bearing 786-O tumors implanted in the sub-renal capsule were treated for 5 days with 30 or 60 mg/kg of sorafenib or vehicle control. Three hours after the last dose, tumors were removed and processed for immunohistochemical analysis, as described in Materials and methods. Tumor sections were stained for **a** Ki-67 or **b** phospho-ERK (pERK) using DAB chromagen and representative photographs were taken using bright-field microscopy (×10). There was no significant change in pERK or Ki-67 in sorafenib-treated tumors compared to those treated with vehicle

in situ (data not shown). However, we cannot rule out effects of sorafenib on inhibition of RAF/MEK/ERK signaling linked to inhibition of endothelial cell survival. It would be interesting to determine to what extent RAF inhibition in endothelial cells and pericytes contributed to the potent inhibition of angiogenesis observed with sorafenib. The use of a selective RAF kinase inhibitor will help answer this question.

On the clinical front, recently, Jain et al. [23] highlighted some of the clinical findings of phase III trials with therapeutic agents targeting VEGF. Based on clinical trials conducted thus far, selective inhibitors of VEGF have not shown significant survival benefit as single agents. However, significant synergies have been observed when given in combination with other therapeutic agents, leading to a substantial clinical benefit. Indeed, bevacizumab, an anti-VEGF monoclonal antibody, when administered as monotherapy, did not increase patient survival, when compared to current standard of care. However, when given in combination with standard chemotherapy, a significant survival benefit was observed [19, 20, 23]. Given that most solid tumors harbor multiple genetic and epigenetic alterations leading to dysregulation of multiple pathways and cellular processes, it seems logical that a multi-target therapy would be more efficacious. Indeed, multi-kinase inhibitors, such as sorafenib and sunitinib, which target multiple signaling pathways upregulated in tumor proliferation and tumor angiogenesis, showed an increase in progression-free survival (PFS) when administered as monotherapy in RCC patients [1123]. While the results from the initial trials are encouraging, further clinical trials will have to be undertaken to fully understand the clinical benefits of multi-kinase inhibitors as single agents and in combination with chemotherapy and radiation.

It has been proposed that one of the mechanisms by which anti-vascular agents mediate their effect is to transiently "normalize" tumor vasculature, resulting in enhanced delivery of oxygen, nutrients, and chemotherapeutic agents [22]. The results of our studies however, show that administration of sorafenib results in a decrease of vasculature, leading to elevated level of tumor hypoxia within 3 days of treatment. The enhanced tumor hypoxia appears to be due to the collapse of the neo-vasculature after the loss of endothelial cells and pericytes. Consistent with our results, a recent study by Franco et al. [14] reported a significant elevation of tumor hypoxia following administration of an anti-VEGFR-2 antibody, DC101, observed within 5 days of treatment and persisting throughout the course of treatment. Clearly, further studies aimed to better understand the tumor microenvironment in response to anti-vascular agents are needed. The knowledge gained from these studies will have significant implications on selecting the right chemotherapeutic agent(s) for possible combination and best sequencing regiments in order to maximize the benefit of these new anti-angiogenic therapies.

To summarize, our results show a potent in vivo anti-tumor activity and tumor stabilization when sorafenib is administered orally in either ectopic or orthotopic RCC tumor models that were $VHL^{-/-}$ (768-O) or $VHL^{+/+}$ (Renca). Analysis of sorafenib-treated tumors revealed that inhibition of VEGF and PDGF-mediated survival of endothelial cells and pericytes represents the predominant mechanism of action leading to the observed tumor growth inhibition. The next step will be to examine tumor biopsies to determine whether similar mechanism of action is observed in RCC patients responding to sorafenib therapy.

Acknowledgments We thank our colleagues at Bayer for technical expertise and support.

References

1. Alavi A, Hood JD, Frausto R, Stupack DG, Cheresh DA (2003) Role of Raf in vascular protection from distinct apoptotic stimuli. Science 301:94–96
2. Amato RJ (2005) Renal cell carcinoma: review of novel single-agent therapeutics and combination regimens. Ann Oncol 16:7–15
3. An J, Fisher M, Rettig MB (2005) VHL expression in renal cell carcinoma sensitizes to bortezomib (PS-341) through an NF-kappaB-dependent mechanism. Oncogene 24:1563–1570
4. Benjamin LE, Hemo I, Keshet E (1998) A plasticity window for blood vessel remodelling is defined by pericyte coverage of the preformed endothelial network and is regulated by PDGF-B and VEGF. Development 125:1591–1598
5. Benjamin LE, Golijanin D, Itin A, Pode D, Keshet E (1999) Selective ablation of immature blood vessels in established human tumors follows vascular endothelial growth factor withdrawal. J Clin Invest 103:159–165
6. Bergers G, Song S, Meyer-Morse N, Bergsland E, Hanahan D (2003) Benefits of targeting both pericytes and endothelial cells in the tumor vasculature with kinase inhibitors. J Clin Invest 111:1287–1295
7. Carlomagno F, Anaganti S, Guida T, Salvatore G, Troncone G, Wilhelm SM, Santoro M (2006) BAY 43–9006 inhibition of oncogenic RET mutants. J Natl Cancer Inst 98:326–334
8. Clark JW, Eder JP, Ryan D, Lathia C, Lenz HJ (2005) Safety and pharmacokinetics of the dual action Raf kinase and vascular endothelial growth factor receptor inhibitor, BAY 43–9006, in patients with advanced, refractory solid tumors. Clin Cancer Res 11:5472–5480
9. Coppin C, Porzsolt F, Awa A, Kumpf J, Coldman A, Wilt T (2005) Immunotherapy for advanced renal cell cancer. Cochrane Database Syst Rev:CD001425
10. Ebbinghaus SW, Gordon MS (2004) Renal cell carcinoma: rationale and development of therapeutic inhibitors of angiogenesis. Hematol Oncol Clin North Am 18:1143–1159, ix–x

11. Escudier B, Szczylik C, Eisin T, Stadler W, Schwartz B, Shan M, Bukowski R (2005) Randomized phase III trial of the multi-kinase inhibitor sorafenib (BAY 43–9006) in patients with advanced renal cell carcinoma (RCC). Eur. J. Cancer Supplements 3:226
12. Ferrara N, Kerbel RS (2005) Angiogenesis as a therapeutic target. Nature 438:967–974
13. Figlin RA (1999) Renal cell carcinoma: management of advanced disease. J Urol 161:381–6; discussion 386–387
14. Franco M, Man S, Chen L, Emmenegger U, Shaked Y, Cheung AM, Brown AS, Hicklin DJ, Foster FS, Kerbel RS (2006) Targeted anti-vascular endothelial growth factor receptor-2 therapy leads to short-term and long-term impairment of vascular function and increase in tumor hypoxia. Cancer Res 66:3639–3648
15. Godley PA, Taylor M (2001) Renal cell carcinoma. Curr Opin Oncol 13:199–203
16. Gore ME, Escudier B (2006) Emerging efficacy endpoints for targeted therapies in advanced renal cell carcinoma. Oncology (Williston Park) 20:19–24
17. Holash J, Wiegand SJ, Yancopoulos GD (1999) New model of tumor angiogenesis: dynamic balance between vessel regression and growth mediated by angiopoietins and VEGF. Oncogene 18:5356–5362
18. Hood JD, Bednarski M, Frausto R, Guccione S, Reisfeld RA, Xiang R, Cheresh DA (2002) Tumor regression by targeted gene delivery to the neovasculature. Science 296:2404–2407
19. Hurwitz H (2004) Integrating the anti-VEGF-A humanized monoclonal antibody bevacizumab with chemotherapy in advanced colorectal cancer. Clin Colorectal Cancer 4(Suppl 2):S62–S68
20. Hurwitz H, Fehrenbacher L, Novotny W, Cartwright T, Hainsworth J, Heim W, Berlin J, Baron A, Griffing S, Holmgren E, Ferrara N, Fyfe G, Rogers B, Ross R, Kabbinavar F (2004) Bevacizumab plus irinotecan, fluorouracil, and leucovorin for metastatic colorectal cancer. N Engl J Med 350:2335–2342
21. Jain RK (2003) Molecular regulation of vessel maturation. Nat Med 9:685–693
22. Jain RK (2005) Normalization of tumor vasculature: an emerging concept in antiangiogenic therapy. Science 307:58–62
23. Jain RK, Duda DG, Clark JW, Loeffler JS (2006) Lessons from phase III clinical trials on anti-VEGF therapy for cancer. Nat Clin Pract Oncol 3:24–40
24. Josko J, Mazurek M (2004) Transcription factors having impact on vascular endothelial growth factor (VEGF) gene expression in angiogenesis. Med Sci Monit 10:RA89–RA98
25. Karasarides M, Chiloeches A, Hayward R, Niculescu-Duvaz D, Scanlon I, Friedlos F, Ogilvie L, Hedley D, Martin J, Marshall CJ, Springer CJ, Marais R (2004) B-RAF is a therapeutic target in melanoma. Oncogene 23:6292–6298
26. Kim JH, Jung CW, Cho YH, Lee J, Lee SH, Kim HY, Park J, Park JO, Kim K, Kim WS, Park YS, Im YH, Kang WK, Park K (2005) Somatic VHL alteration and its impact on prognosis in patients with clear cell renal cell carcinoma. Oncol Rep 13:859–864
27. Mancuso A, Sternberg CN (2005) New treatments for metastatic kidney cancer. Can J Urol 12 Suppl 1: 66–70; discussion 105
28. Motzer RJ, Mazumdar M, Bacik J, Russo P, Berg WJ, Metz EM (2000) Effect of cytokine therapy on survival for patients with advanced renal cell carcinoma. J Clin Oncol 18:1928–1935
29. Na X, Wu G, Ryan CK, Schoen SR, di'Santagnese PA, Messing EM (2003) Overproduction of vascular endothelial growth factor related to von Hippel-Lindau tumor suppressor gene mutations and hypoxia-inducible factor-1 alpha expression in renal cell carcinomas. J Urol 170:588–592
30. Salvatore G, De Falco V, Salerno P, Nappi TC, Pepe S, Troncone G, Carlomagno F, Melillo RM, Wilhelm SM, Santoro M (2006) BRAF is a therapeutic target in aggressive thyroid carcinoma. Clin Cancer Res 12:1623–1629
31. Shaheen PE, Bukowski RM (2005) Emerging drugs for renal cell carcinoma. Expert Opin Emerg Drugs 10:773–795
32. Sharma A, Trivedi NR, Zimmerman MA, Tuveson DA, Smith CD, Robertson GP (2005) Mutant V599EB-Raf regulates growth and vascular development of malignant melanoma tumors. Cancer Res 65:2412–2421
33. Shinojima T, Oya M, Takayanagi A, Mizuno R, Shimizu N, Murai M (2006) Renal cancer cells lacking hypoxia inducible factor (HIF)-1{alpha} expression maintain vascular endothelial growth factor expression through HIF-2{alpha}. Carcinogenesis
34. Turner KJ, Moore JW, Jones A, Taylor CF, Cuthbert-Heavens D, Han C, Leek RD, Gatter KC, Maxwell PH, Ratcliffe PJ, Cranston D, Harris AL (2002) Expression of hypoxia-inducible factors in human renal cancer: relationship to angiogenesis and to the von Hippel-Lindau gene mutation. Cancer Res 62:2957–2961
35. Wilhelm SM, Carter C, Tang L, Wilkie D, McNabola A, Rong H, Chen C, Zhang X, Vincent P, McHugh M, Cao Y, Shujath J, Gawlak S, Eveleigh D, Rowley B, Liu L, Adnane L, Lynch M, Auclair D, Taylor I, Gedrich R, Voznesensky A, Riedl B, Post LE, Bollag G, Trail PA (2004) BAY 43–9006 exhibits broad spectrum oral antitumor activity and targets the RAF/MEK/ERK pathway and receptor tyrosine kinases involved in tumor progression and angiogenesis. Cancer Res 64:7099–7109